Heliyon 5 (2019) e02807

Contents lists available at ScienceDirect

Heliyon

journal homepage: www.heliyon.com

Heliyon

Research article

Optimization of cellulose nanocrystals from bamboo shoots using Response Surface Methodology

Christian J. Wijaya [a,b], Suryadi Ismadji [b], Hakun W. Aparamarta [a], Setiyo Gunawan [a,*]

[a] Department of Chemical Engineering, Faculty of Industrial Technology, Institut Teknologi Sepuluh Nopember, Keputih Sukolilo, Surabaya, 60111, Indonesia
[b] Department of Chemical Engineering, Widya Mandala Surabaya Catholic University, Kalijudan 37, Surabaya, 60114, Indonesia

ARTICLE INFO

Keywords:
Chemical engineering
Materials science
Acid hydrolysis
Bamboo shoots
Cellulose nanocrystals
Optimization

ABSTRACT

Cellulose-based advanced materials, such as cellulose nanocrystals (CNC), have high potential application for drug delivery system. In this study, the CNC were produced from bamboo shoots using acid hydrolysis process. The delignification of bamboo shoots was conducted using alkali and hydrogen peroxide pretreatment processes. The operating condition of the production of CNC from bamboo shoots was optimized using Response Surface Methodology (RSM) based on the yield and crystals recovery as the responses. The optimum CNC yield of 50.67 ± 0.74% with a crystals recovery of 77.99 ± 1.14% was obtained at the sulfuric acid concentration of 54.73 wt% and a temperature of 39 °C from the optimization based on the yield. This optimization has been validated to confirm the accuracy.

1. Introduction

Bamboo is a rapidly growing plant that is widely cultivated in Asia, including Indonesia. The shoots of this plant are edible and used as one of the important ingredients of domestic foods. Bamboo shoots (BS) have a unique characteristic; their odor is unpleasant and pungent. BS are lignocellulosic material, which consists of lignin, hemicelluloses, and cellulose. The compositions based on the dry matter of BS were 5–11% of lignin, 24–27% of hemicelluloses, and 23–35% of cellulose (Li et al., 2015).

In recent years, the research interests of BS are mainly on the polysaccharides constituents (Chen et al., 2018a,b; Chen et al., 2018a,b; He et al., 2016; Zhang et al., 2018), the bioactive agents contents like antioxidant, phenolic compound, and angiotensin converting enzyme inhibition activity (Gong et al., 2016; Park and Jhon, 2010), and the pyrolysis products of BS (Ye et al., 2015). As compared to the other lignocellulosic materials, the cellulose content of BS is relatively high, while the low lignin content facilitates the easy treatment to extract the cellulose content. So far, the utilization of BS as the raw material for cellulose nanocrystals (CNC) production has never been studied.

Cellulose nanocrystals (CNC) are one of the advanced cellulose-based materials. CNC are an advanced nano-scale material with a needle or rod-like crystals structure. CNC have a diameter size of 5 nm up to 30 nm and length size of 100 nm up to several μm. CNC possess good physical characteristics as well as their chemical characteristics, such as reactive hydroxyl groups, high crystallinity, large surface area, good thermal stability, good mechanical properties, biocompatible, biodegradable, and non-toxic (Collazo-Bigliardi et al., 2018; Qing et al., 2016; Zainuddin et al., 2017). Due to their excellence properties, CNC can be used for advanced utilization such as drug delivery, tissue engineering, composite material, protein or enzyme immobilization, emulsifier, and others nanomaterial synthesis (Wijaya et al., 2017). Previous studies have reported the CNC production from various natural resources, such as rice straw (Lu and Hsieh, 2012), corncob (Silvério, et al., 2013), sugarcane bagasse (Teixeira et al., 2011), sugar palm fiber (Ilyas et al., 2018), sago seed shell (Naduparambath et al., 2018; Naduparambath and Purushothaman, 2016), passion fruit peels (Wijaya et al., 2017), and groundnut shell (Bano and Negi, 2017). The cellulose content of BS also can be converted to micro- and nano-scale material, such as CNC, and currently there is no study utilizes the BS for the CNC production and its subsequent use as a drug carrier in drug delivery system.

CNC can be produced using various methods, such as steam explosion treatment (Abraham et al., 2011; Cherian et al., 2010; Deepa et al., 2011), ionic liquids (Man et al., 2011; Tan et al., 2015), ultrasound technique (Li et al., 2012b), high pressure homogenization (Kawee et al., 2018; Lee et al., 2018; Li et al., 2012a; Wang et al., 2015), acid hydrolysis (Coelho et al., 2018; Collazo-Bigliardi et al., 2018; Gu et al., 2017; Robles et al., 2018), enzymatic hydrolysis (Chen et al., 2018c; Henriksson et al.,

* Corresponding author.
E-mail address: gunawan@chem-eng.its.ac.id (S. Gunawan).

https://doi.org/10.1016/j.heliyon.2019.e02807
Received 9 April 2019; Received in revised form 29 July 2019; Accepted 7 November 2019

2007), and combined treatments. Acid hydrolysis is the most popular and common method for CNC production. The advantages of this method are its simplicity and the convenient removal process of the amorphous cellulose region using acid solution (Phanthong et al., 2018). Sulfuric acid is the most common acid solution used to produce CNC with a negative charge, which stable in suspension (Gu et al., 2017).

In this study, the preparation of CNC from BS was conducted using acid hydrolysis method, and sulfuric acid was used as the hydrolyzing agent. The optimization of the acid hydrolysis process was also studied using Response Surface Methodology (RSM) to determine the optimum conditions of the recovery of CNC from BS.

2. Experimental

2.1. Materials

Bamboo shoots (*Dendrocalamus asper*) were obtained from the local market in Surabaya, East Java, Indonesia. BS were harvested after having a height of 30–50 cm from the ground. BS were repeatedly washed and thinly sliced before they were dried under sunlight for three days. Dried BS were ground and sieved through a 100-mesh sieve. All chemicals, i.e., sodium hydroxide, hydrogen peroxide (50%), and sulfuric acid (98%), were purchased from Sigma-Aldrich (Singapore) as an analytical grade.

2.2. Pretreatment of BS

Cellulose from BS was obtained by the following steps: delignification and bleaching steps. For the delignification process, BS powder (10 g) were soaked using 200 mL of 20% (w/v) sodium hydroxide solution. The mixture was heated at 90 °C for 4 h under continuous stirring. The solid residue was washed with distilled water until the pH was neutral. Then, it was dried using oven at 50 °C for overnight. For the bleaching process, the dried residue was soaked using 4% (w/v) sodium hydroxide solution at 50 °C under continuous stirring. Then, 50% hydrogen peroxide with the same volume of sodium hydroxide was added dropwise. The bleaching process was done for 60 min under continuous stirring. The pretreated bamboo shoots (PBS) were washed with distilled water until neutral pH and then dried at 50 °C for overnight.

2.3. Isolation of CNC

CNC were isolated from the cellulose of BS by acid hydrolysis process. The acid hydrolysis process was carried out using different concentrations of sulfuric acid (45, 55, 65, and 75 wt%) at various temperatures (30, 45, and 60 °C) for 60 min. The PBS mass to sulfuric acid volume ratio was 1:20. After the hydrolysis process completed, excess cold distilled water was added to the mixture to stop the hydrolysis process. The suspension was centrifuged at 6000 rpm for 10 min to remove the acid solution. The precipitate was washed using distilled water until neutral pH was reached. The neutral suspension was sonicated in an ice bath for 20 min and dried using freeze dryer at a pressure of 0.08 mbar and temperature of –42 °C.

2.4. Characterizations

2.4.1. Determination of chemical composition

The chemical compositions of BS and PBS, such as the hot water soluble, lignin, hemicelluloses, and cellulose content, were determined at different stages of treatment (Datta, 1981). 1 g of sample was refluxed with 150 mL of distilled water at 100 °C for 2 h to remove hot water soluble content. The dried solid residue was then refluxed with 150 mL of 0.5 M sulfuric acid solution at 100 °C for 2 h to remove hemicelluloses content. After that, the dried solid residue was treated with 10 mL of 72% (v/v) sulfuric acid solution at room temperature for 4 h. Then, it was diluted to 0.5 M sulfuric acid solution and refluxed at 100 °C for 2 h to remove cellulose content. The ash content was determined using furnace at a temperature of 600 °C for 6 h, while the weight loss during furnacing was the lignin content. The moisture content was determined using moisture balance.

2.4.2. Thermal gravimetric analysis (TGA)

The material stability under thermal condition was analyzed using a Perkin Elmer Diamond TG/DTA thermal analyzer. The TGA analysis was carried out in a nitrogen gas flow of 150 mL/min with a constant heating and cooling rate of 10 °C/min at a temperature range of 25–600°.

2.4.3. X-ray diffraction (XRD) analysis

The crystallinity of CNC was analyzed using PANalytical X'Pert PRO X-ray diffractometer with a monochromated high-intensity Cu Kα radiation (1.5406 Å) operating at 40 kV and 30 mA. The XRD pattern was recorded using a step size of 0.02°/C at the angle range of 5–60°. The crystallinity index percentage was expressed by this equation below (Ditzel et al., 2017):

$$CrI = [1 - (I_{am} / I_{200})] \times 100\% \quad (1)$$

where I_{am} is the minimum value of the 110 and 200 lattices diffractions which exhibits the amorphous region, while I_{200} is the maximum value of the 200 lattice which exhibits the total of amorphous and crystalline regions (Wijaya et al., 2017).

2.4.4. Scanning electron microscopy (SEM) analysis

The SEM analysis was used to observe the microstructure of CNC. A fine auto coater (JFC-1200, JEOL, Ltd., Japan) was used to coat the material using a thin conductive platinum layer under argon atmosphere. The SEM analysis was carried out using a JEOL JSM-6390 field emission SEM that was operated at an accelerating voltage of 5 kV.

2.4.5. Fourier transform infrared spectroscopy (FTIR) analysis

The FTIR analysis was used to determine the functional groups in the BS, PBS, and CNC. The change of the functional groups based on the treatments was used to know the effects of the treatments on the material's structure. The FTIR analysis was carried out using FTIR Shimadzu 8400S that used KBr in pelleting the materials. The spectra were recorded at the wavenumber range of 4000–400 cm^{-1}.

2.5. Optimization

RSM was used to analyze the optimum condition of the acid hydrolysis process in the CNC production, and Minitab 16 statistical software (Minitab Inc., ITS Surabaya, Indonesia) was employed for this purpose. RSM was also used to describe the significance of the independent variables toward the response, where the significance was determined when the p-value < 0.05. The central composite design with two independent variables (sulfuric acid concentration and temperature) was used for the optimization. Based on the full factorial design with two repetitions, 24 independent experiments were carried out. The influence of independent variables toward the response is given by the following equation (Muthukumaran et al., 2018):

$$Y_{response} = \alpha_0 + \sum \alpha_i X_i + \sum \alpha_{ii} X_i^2 + \sum \alpha_{ij} X_i X_j \quad (2)$$

where α_0 is the constant, while α_i, α_{ii}, and α_{ij} are the linear, square, and interaction effects coefficient of the two independent variables. Here, X_i and X_j indicate the independent variables used in this research.

As the responses in this statistical analysis are the yield of CNC and the crystals recovery of CNC from PBS. The yield and crystals recovery of CNC was calculated by these following equations:

$$\%\ Yield = (m_{CNC} / m_{PBS}) \times 100\% \quad (3)$$

$$\%\ Crystals\ Recovery = (mc_{CNC} / mc_{PBS}) \times 100\% \quad (4)$$

$$mc_{CNC} = CrI\%_{CNC} \times m_{CNC} \quad (5)$$

$$mc_{PBS} = CrI\%_{PBS} \times m_{PBS} \quad (6)$$

where m_{CNC} and mc_{CNC} are the mass and the crystals mass of CNC, while m_{PBS} and mc_{PBS} are the mass and the crystals mass of PBS, respectively. $CrI\%_{CNC}$ and $CrI\%_{PBS}$ are the crystallinity index of CNC and PBS, respectively.

3. Results and discussions

3.1. Cellulose from BS

The chemical compositions of BS and their pretreated form are presented in Table 1. The compositions of BS are consistent with the previous studies; they have high cellulose and low lignin content. With high cellulose content indicates that BS are very potential the raw material for CNC production. The change of chemical composition between BS and their pretreated form is obvious as seen in Table 1. After the pretreatment, the cellulose content significantly increases from 33.14 ± 0.34% to 74.34 ± 0.40%, while a significant decrease of the hemicelluloses and lignin contents is observed. The reduction of lignin content from 9.72 ± 0.45% to 0.63 ± 0.41% makes the subsequent process (acid hydrolysis) become easier.

Fig. 1 shows the thermal decomposition behavior of BS and PBS, a substantial weight loss of both materials during the heating process is observed. In the temperature range of 35–150 °C, the evaporation of moisture content occurred as detected by the weight loss, while the cellulose content was degraded at the temperature range of 220–365 °C. In the TGA curve of PBS, the substantial weight loss is observed in a temperature region that indicates the degradation of a significant amount of cellulose in PBS. The maximum degradation of cellulose was achieved at temperature of 325.3 °C. This phenomenon supports the result in Table 1. Due to the hemicelluloses and lignin reduction by the pretreatment process, the curve region of hemicelluloses and lignin are not seen in the PBS curve that means that the hemicelluloses and lignin contents are low enough. This phenomenon indicates that the pretreatment process was successful.

3.2. Isolation of CNC from PBS

XRD analysis was conducted for every product of the acid hydrolysis process. The XRD patterns of CNC were displayed in Fig. 2, and matched up with the standard of the cellulose I crystals (JCPDS No. 00-050-22411). The XRD pattern of CNC has fours existed peaks at 2θ of 15.5°, 16.4°, 22.8°, and 35° assigned to the $1\tilde{1}0$, 110, 200, and 004 planes, respectively. The crystallinity index was calculated using Eq. (1), where the result of PBS was 53.15%, and the highest result of CNC was 84.55%. The results indicate that the acid hydrolysis process successfully removes the amorphous region of PBS. The BS-CNC crystallinity index is high enough compared to the CNC isolated from other natural materials, such as from rice husk (CrI = 90%), coffee husk (CrI = 92%) (Collazo-Bigliardi et al., 2018), blue agave waste (CrI = 85–88%) (Tang et al., 2017), sugar palm fibres (CrI = 85.90%) (Ilyas et al., 2018), eucalyptus cellulose (CrI = 75%) (Gu et al., 2017), sago seed shells (CrI = 69%) (Naduparambath et al., 2018), and elephant grass (CrI = 72–77%) (Nascimento and Rezende, 2018). The crystallinity index of the CNC depends on the amount of cellulose crystals region in the raw material. Several natural resources, like kinds of husk, have higher amount of cellulose crystals region compared to any kind of shoots or grass. Therefore, the crystallinity index of the CNC from BS is lower than the CNC from rice husk and coffee husk.

Table 1
The chemical composition of BS and its pretreated form.

Component (in wt%)	This study		BS		
	BS	PBS	Ref[a]	Ref[b]	Ref[c]
Moisture	12.85 ± 0.10	6.95 ± 0.17	-	-	-
Hot water soluble	12.71 ± 0.56	3.29 ± 0.37	-	-	-
Hemicelluloses	22.79 ± 1.09	4.82 ± 0.18	21.3	24.8	13.0
Cellulose	33.14 ± 0.34	74.34 ± 0.40	22.8	27.5	31.1
Lignin	9.72 ± 0.45	0.63 ± 0.41	1.8	5.2	5.3
Ash	8.79 ± 0.42	9.98 ± 0.18	-	-	-

[a] (Yang et al., 2014).
[b] (Li et al., 2015).
[c] (Chang et al., 2013).

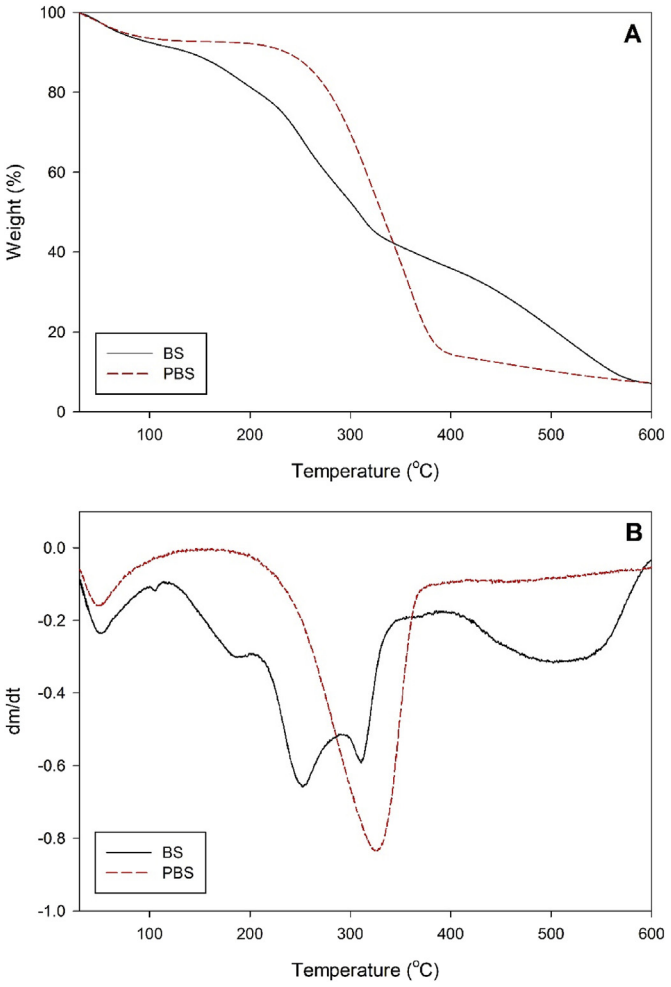

Fig. 1. TGA (A) and DTG (B) curves of bamboo shoots and its pretreated form.

The crystallinity index was used for the calculation of the yield of CNC (Eq. 3), and the crystals recovery of CNC (Eq. 4). The yields and crystals recoveries of CNCs are summarized in Table 2. At the sulfuric acid concentration of 65 wt% and temperature of 45 °C, the highest yield and crystals recovery of CNC were 51.86 ± 2.04% and 82.50 ± 3.24%, respectively. The high crystals recovery of CNC indicates that the amorphous region was hydrolyzed into sugars while the crystalline region remains intact. At higher sulfuric acid concentration (75 wt%), both of amorphous and crystalline region of cellulose were hydrolyzed into sugars.

The morphology of CNC from BS is depicted in Fig. 3. The interconnected rod-like structure of the CNC has been proven by this SEM figure. The interconnected crystals structure makes CNC has high stability in suspension. The sonication treatment also assists the cavitation of CNC so that it is less precipitated in suspension by the formation of interconnected nano-scale cellulose structure.

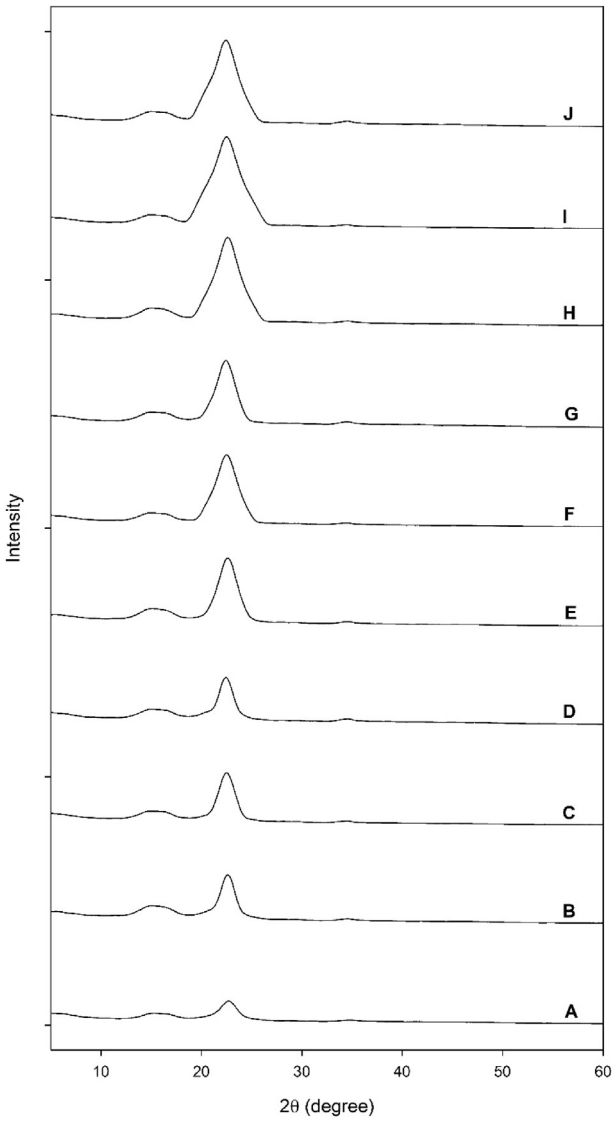

Fig. 2. The XRD patterns of pretreated bamboo shoots (A) and CNCs which produced by acid hydrolysis process using [H_2SO_4] of 45 wt% at temperatures of 30 °C (B), 45 °C (C), and 60 °C (D); using [H_2SO_4] of 55 wt% at temperatures of 30 °C (E), 45 °C (F), and 60 °C (G); and using [H_2SO_4] of 65 wt% at temperatures of 30 °C (H), 45 °C (I), and 60 °C (J).

Table 2
The yields and crystals recoveries of CNCs in every combined variables.

Yields of CNC (%)				
Temp. (°C)	[H_2SO_4] (wt%)			
	45	55	65	75
30	42.97 ± 1.00	41.14 ± 0.58	48.45 ± 2.67	n.d.
45	41.78 ± 0.60	40.79 ± 0.19	51.86 ± 2.04	n.d.
60	40.30 ± 0.45	39.88 ± 0.56	40.22 ± 1.51	n.d.
Crystals recoveries of CNC (%)				
Temp. (°C)	[H_2SO_4] (wt%)			
	45	55	65	75
30	51.37 ± 1.19	57.89 ± 0.82	71.31 ± 3.93	n.d.
45	57.48 ± 0.82	61.69 ± 0.29	82.50 ± 3.24	n.d.
60	49.87 ± 0.56	57.54 ± 0.81	60.30 ± 2.27	n.d.

n.d.: not detected.

The functional groups of BS, PBS, and CNC have been analyzed using FTIR method, and the spectra are shown in Fig. 4. The appearance of O–H, C–H, and C–O stretching vibration peaks at 3337 cm^{-1}, 2890 cm^{-1}, and 1045 cm^{-1}, respectively, represents the cellulose content in all of the samples, (Gu et al., 2017; Hernandez et al., 2018). The peak of O–H stretching vibration in the CNC has stronger transmittance compared to PBS and BS samples. The intensity of this hydrogen bonding increase is due to the removal of some parts of the amorphous region and the breakdown of some β-glycosidic bonds in the cellulose structure. The removal of some parts of the amorphous region is supported by the peak reduction of CH_2 bonding at the sixth C in the cyclic chain of glucose (at a wavenumber of 1325 cm^{-1}). The peak at 897 cm^{-1} indicates the β-glycosidic linkage between the monomers of cellulose (Naduparambath et al., 2018). The absorbed water of all samples is observed at the wavenumber of 1647 cm^{-1} (Xing et al., 2018).

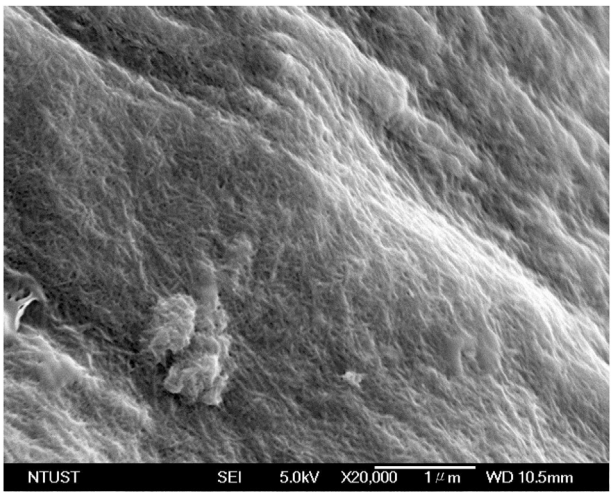

Fig. 3. Scanning electron microscopy of CNC.

The success of the pretreatment process is indicated by the reduction of lignin and hemicelluloses content in the BS and PBS samples. The aromatic skeletal vibration of lignin is shown at 1516 cm^{-1}, while the C=O and C–O stretching of hemicelluloses are at 1729 cm^{-1} and 1264 cm^{-1}, respectively (Xing et al., 2018). In the FTIR spectrum of PBS, the peak that correspond to lignin could not be observed, a strong indication that the lignin content is low. While, the peaks transmittance correspond to hemicelluloses are significantly reduced. After the acid hydrolysis process, the hemicelluloses peaks in the FTIR spectra of CNC disappear completely due to the breakdown of hemicelluloses into pentose sugars. The C–H bonds of the crystalline cellulose is indicated by the vibrations at 1379-1311 cm^{-1} (Hernandez et al., 2018). In the FTIR spectra of CNC, the S=O and C–O–S vibrations at 1250 cm^{-1} and 833 cm^{-1}, respectively, could not be detected which indicates the CNC contains low sulfur content (Gu et al., 2017; Xing et al., 2018).

3.3. Response surface methodology

3.3.1. Model fitting

The regression coefficients along with the Fisher value (*F*-value) and probability (*p*-value) of the model fitting are given in Table 3. The *F*-value and *p*-value are used to specify the fitness and significance of the model fitting. From the *F*-value, the statistical significance is considered if the *F*-value is higher than the critical *F*-value at a level of 5%. The significance of each fitting parameter toward the response value is also determined by the *p*-value < 0.05. The significance parameter is the sulfuric acid concentration as the independent variable for acid hydrolysis process. Therefore, the mathematical models for the yield and crystals recovery of CNC are given by the following equations:

$$Yield\ \ of\ \ CNC = -305.108 + 12.526\,[H_2SO_4] - 0.114\,[H_2SO_4]^2 \quad (7)$$

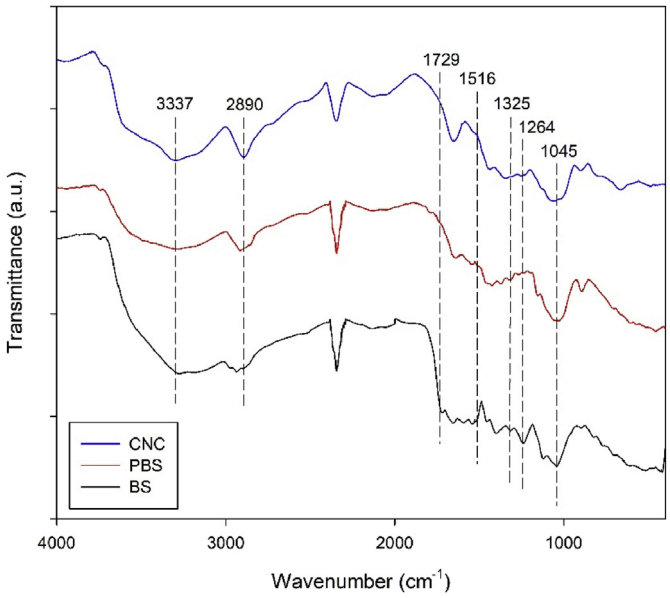

Fig. 4. FTIR spectra of bamboo shoots, pretreated bamboo shoots, and CNC.

Table 3
Regression coefficients, *F*-value, and *p*-values (significance levels) for the yield and crystals recovery of CNC as the responses.

Parameter	The yield of CNC (%)			Crystals recovery of CNC (%)		
	Coefficient	*F*-value	*p*-value	Coefficient	*F*-value	*p*-value
α_0	-305.108	22.22	0.001	-597.725	20.65	0.000
α_1	12.526	36.17	0.000	21.879	48.44	0.000
α_2	0.674	0.18	0.678	2.779	1.32	0.266
α_{11}	-0.114	46.95	0.000	-0.194	59.11	0.000
α_{22}	-0.009	0.32	0.581	-0.031	1.66	0.214
α_{12}	0.000	0.00	0.978	-0.002	0.01	0.912

α_0 = constant; α_1 = $[H_2SO_4]$ (linear parameter); α_2 = temperature (linear parameter); α_{11} = $[H_2SO_4]^2$ (quadratic parameter); α_{22} = temperature^2 (quadratic parameter); and α_{12} = $[H_2SO_4]$ × temperature (interaction parameter).

$$Crystals\ recovery\ of\ CNC = -597.725 + 21.879\,[H_2SO_4] - 0.194\,[H_2SO_4]^2 \quad (8)$$

3.3.2. *Effects of sulfuric acid concentration and temperature on the yield and crystals recovery of CNC*

The contour plots of the yield and crystals recovery of CNC are shown in Fig. 5. Fig. 5A describes the effect of sulfuric acid concentration towards the yield of CNC. These contour plots are also used to attest the model fitting results about the significance of both variables. In the range of 45–75 wt%, the yield of CNC is found to be very varied, The yield of CNC >50% was obtained around 55 wt% of the sulfuric acid concentration. At a sulfuric acid concentration higher or lower than 55%, the decrease of the yield of CNC is observed. Temperature has no significant influence on the yield of CNC.

For the crystals recovery of CNC, a similar phenomenon was observed. The sulfuric acid concentration has a more significant effect than the temperature as shown in Fig. 5B. The crystals recovery of CNC higher than 70% was obtained at a sulfuric acid concentration around 55–60 wt%. The temperature has no significant effect on the crystals recovery of CNC.

3.3.3. *Optimization of the acid hydrolysis process*

The "Response Optimizer" tool of the Minitab 16 statistical software was used to optimize the acid hydrolysis process for the production of CNC from BS. Both of the independent variables were optimized to satisfy each response which evaluated by the composite desirability value. The value equals to 1 indicates to the very satisfying solution, while 0 indicates that the response is out of the acceptable limits. For both optimizations, the deciding goal was the maximum solution with the lower response value of 0 and the target or upper response value of 100.

As shown in Fig. 6A, the optimum condition is a process using sulfuric acid concentration of 54.73 wt% at a temperature of 39 °C, where the maximum yield of CNC reaches 51.30%. The composite desirability of 0.51 indicates that only a part of the optimized solution satisfies the goal of this optimization. While for the crystals recovery of CNC as shown in Fig. 6B, the sulfuric acid concentration of 56.21 wt% and the temperature of 43 °C is the optimum condition, with the crystals recovery of CNC was 77.48%. This optimized solution has high satisfaction due to its composite desirability of 0.77.

Acid hydrolysis process was conducted under the optimum condition to validate the optimization results as shown in Table 4. Based on their optimum condition, the yield of CNC obtained was 50.67 ± 0.74% with an error of 1.21%, while the crystals recovery of CNC was 76.25 ± 1.93% with an error of 1.60%. It indicates the high accuracy of the optimization results. From the optimization based on yield, CNC have CrI of 81.80%, while it is 83.65% from the optimization based on crystals recovery. This CrI indicates the quantitative indicator of crystallinity, which means the high CrI represents the high crystallinity of this CNC. The enhancement of CrI affects the hardness, density, transparency, and diffusion of the

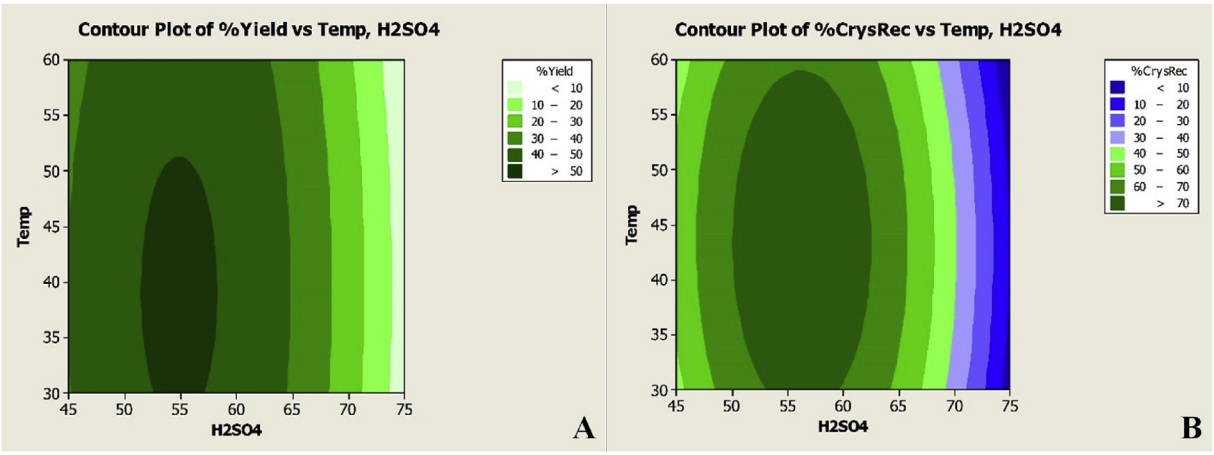

Fig. 5. The contour plots for the yield (A) and crystals recovery (B) of CNC.

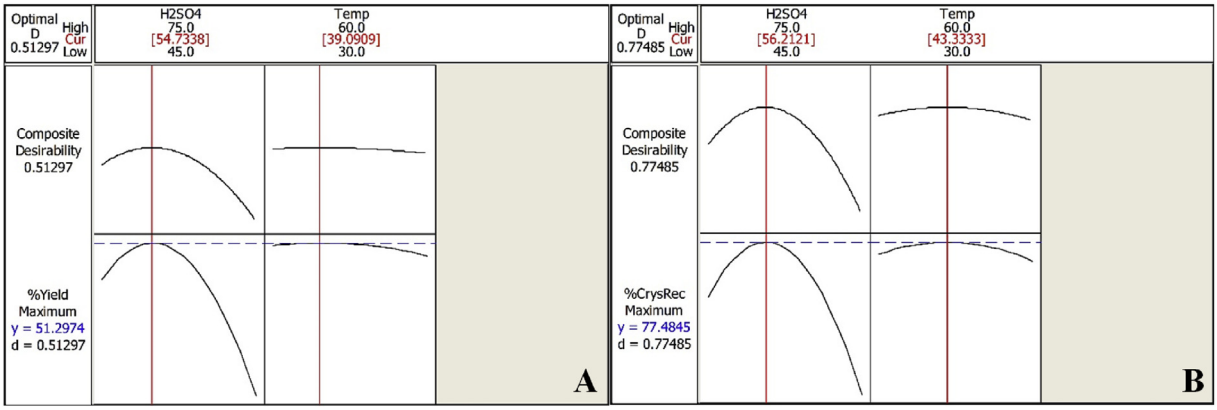

Fig. 6. Optimization results for the yield (A) and crystals recovery (B) of CNC.

Table 4
Validation of the optimization results.

Optimization	Validation results		
	CrI (%)	Yield of CNC (%)	Crystals recovery of CNC (%)
Based on yield[a]	81.80	50.67 ± 0.74%	77.99 ± 1.14%
Based on crystals recovery[b]	83.65	48.44 ± 1.23%	76.25 ± 1.93%

[a] using sulfuric acid concentration of 54.73 wt% at a temperature of 39 °C.
[b] using sulfuric acid concentration of 56.21 wt% at a temperature of 43 °C.

material.

4. Conclusion

This study utilized bamboo shoots (BS), a potential lignocellulosic material with high enough cellulose content and low lignin content, as the raw material for the production of CNC. The CNC have the structure of the rod-like crystals. In this CNC production, the crystals recovery of 77.99 ± 1.14% and the yield of 50.67 ± 0.74% were obtained using a sulfuric acid concentration of 54.73% and a temperature of 39 °C. As the results, CNC from BS have a potential application for composite material, drug delivery, emulsifier, enzyme immobilization, nanomaterial synthesis, and tissue engineering.

Declarations

Author contribution statement

Christian J. Wijaya: Conceived and designed the experiments; Performed the experiments; Analyzed and interpreted the data; Wrote the paper.

Suryadi Ismadji, Setiyo Gunawan, Hakun W. Aparamarta: Conceived and designed the experiments; Contributed reagents, material, and analysis tools or data; Analyzed and interpreted the data.

Funding statement

This work was supported by The Directorate General of Resources for Science, Technology, and Higher Education, Ministry of Research, Technology, and Higher Education of Republic Indonesia (No. 851/PKS/ITS/2019) and Widya Mandala Surabaya Catholic University.

Competing interest statement

The authors declare no conflict of interest.

Additional information

No additional information is available for this paper.

References

Abraham, E., Deepa, B., Pothan, L.A., Jacob, M., Thomas, S., Cvelbar, U., Anandjiwala, R., 2011. Extraction of nanocellulose fibrils from lignocellulosic fibres: a novel approach. Carbohydr. Polym. 86 (4), 1468–1475.

Bano, S., Negi, Y.S., 2017. Studies on cellulose nanocrystals isolated from groundnut shells. Carbohydr. Polym. 157, 1041–1049.

Chang, W.J., Chang, M.J., Chang, S.T., Yeh, T.F., 2013. Chemical composition and immunohistological variations of a growing bamboo shoot. J. Wood Chem. Technol. 33 (2), 144–155.

Chen, G., Bu, F., Chen, X., Li, C., Wang, S., Kan, J., 2018a. Ultrasonic extraction, structural characterization, physicochemical properties and antioxidant activities of polysaccharides from bamboo shoots (Chimonobambusa quadrangularis) processing by-products. Int. J. Biol. Macromol. 112, 656–666.

Chen, G., Chen, K., Zhang, R., Chen, X., Hu, P., Kan, J., 2018b. Polysaccharides from bamboo shoots processing by-products: new insight into extraction and characterization. Food Chem. 245 (November 2017), 1113–1123.

Chen, X.Q., Deng, X.Y., Shen, W.H., Jia, M.Y., 2018c. Preparation and characterization of the spherical nanosized cellulose by the enzymatic hydrolysis of pulp fibers. Carbohydr. Polym. 181 (November 2017), 879–884.

Cherian, B.M., Leão, A.L., de Souza, S.F., Thomas, S., Pothan, L.A., Kottaisamy, M., 2010. Isolation of nanocellulose from pineapple leaf fibres by steam explosion. Carbohydr. Polym. 81 (3), 720–725.

Coelho, C.C.S., Michelin, M., Cerqueira, M.A., Gonçalves, C., Tonon, R.V., Pastrana, L.M., et al., 2018. Cellulose nanocrystals from grape pomace: production, properties and cytotoxicity assessment. Carbohydr. Polym. 192 (February), 327–336.

Collazo-Bigliardi, S., Ortega-Toro, R., Chiralt Boix, A., 2018. Isolation and characterisation of microcrystalline cellulose and cellulose nanocrystals from coffee husk and comparative study with rice husk. Carbohydr. Polym. 191 (October 2017), 205–215.

Datta, R., 1981. Acidogenic digestion of lignoselulose-acid yield and conversion of components. Biotechnol. Bioeng. 23, 2167–2170.

Deepa, B., Abraham, E., Cherian, B.M., Bismarck, A., Blaker, J.J., Pothan, L.A., et al., 2011. Structure, morphology and thermal characteristics of banana nano fibers obtained by steam explosion. Bioresour. Technol. 102 (2), 1988–1997.

Ditzel, F.I., Prestes, E., Carvalho, B.M., Demiate, I.M., Pinheiro, L.A., 2017. Nanocrystalline cellulose extracted from pine wood and corncob. Carbohydr. Polym. 157, 1577–1585.

Gong, W., Xiang, Z., Ye, F., Zhao, G., 2016. Composition and structure of an antioxidant acetic acid lignin isolated from shoot shell of bamboo (Dendrocalamus Latiforus). Ind. Crops Prod. 91, 340–349.

Gu, J., Hu, C., Zhong, R., Tu, D., Yun, H., Zhang, W., Leu, S.Y., 2017. Isolation of cellulose nanocrystals from medium density fiberboards. Carbohydr. Polym. 167, 70–78.

He, S., Wang, X., Zhang, Y., Wang, J., Sun, H., Wang, J., et al., 2016. Isolation and prebiotic activity of water-soluble polysaccharides fractions from the bamboo shoots (Phyllostachys praecox). Carbohydr. Polym. 151, 295–304.

Henriksson, M., Henriksson, G., Berglund, L.A., Lindström, T., 2007. An environmentally friendly method for enzyme-assisted preparation of microfibrillated cellulose (MFC) nanofibers. Eur. Polym. J. 43 (8), 3434–3441.

Hernandez, C.C., Ferreira, F.F., Rosa, D.S., 2018. X-ray powder diffraction and other analyses of cellulose nanocrystals obtained from corn straw by chemical treatments. Carbohydr. Polym. 193 (January), 39–44.

Ilyas, R.A., Sapuan, S.M., Ishak, M.R., 2018. Isolation and characterization of nanocrystalline cellulose from sugar palm fibres (Arenga Pinnata). Carbohydr. Polym. 181, 1038–1051.

Kawee, N., Lam, N.T., Sukyai, P., 2018. Homogenous isolation of individualized bacterial nanofibrillated cellulose by high pressure homogenization. Carbohydr. Polym. 179 (October 2017), 394–401.

Lee, M., Heo, M.H., Lee, H., Lee, H.-H., Jeong, H., Kim, Y.-W., Shin, J., 2018. Facile and eco-friendly extraction of cellulose nanocrystals *via* electron beam irradiation followed by high-pressure homogenization. Green Chem. 20 (11), 2596–2610.

Li, J., Wei, X., Wang, Q., Chen, J., Chang, G., Kong, L., et al., 2012a. Homogeneous isolation of nanocellulose from sugarcane bagasse by high pressure homogenization. Carbohydr. Polym. 90 (4), 1609–1613.

Li, K., Wang, X., Wang, J., Zhang, J., 2015. Benefits from additives and xylanase during enzymatic hydrolysis of bamboo shoot and mature bamboo. Bioresour. Technol. 192, 424–431.

Li, W., Yue, J., Liu, S., 2012b. Preparation of nanocrystalline cellulose via ultrasound and its reinforcement capability for poly(vinyl alcohol) composites. Ultrason. Sonochem. 19 (3), 479–485.

Lu, P., Hsieh, Y., 2012. Preparation and characterization of cellulose nanocrystals from rice straw. Carbohydr. Polym. 87 (1), 564–573.

Man, Z., Muhammad, N., Sarwono, A., Bustam, M.A., Vignesh Kumar, M., Rafiq, S., 2011. Preparation of cellulose nanocrystals using an ionic liquid. J. Polym. Environ. 19 (3), 726–731.

Muthukumaran, C., Kanmani, B.R., Sharmila, G., Kumar, M., Shanmugaprakash, M., 2018. Carboxymethylation of pectin: optimization, characterization and in-vitro drug release studies. Carbohydr. Polym. 194 (January), 311–318.

Naduparambath, S., Jinitha, T.V., Shaniba, V., Sreejith, M.P., Balan, A.K., Purushothaman, E., 2018. Isolation and characterisation of cellulose nanocrystals from sago seed shells. Carbohydr. Polym. 180 (April 2017), 13–20.

Naduparambath, S., Purushothaman, E., 2016. Sago seed shell: determination of the composition and isolation of microcrystalline cellulose (MCC). Cellulose 23 (3), 1803–1812.

Nascimento, S.A., Rezende, C.A., 2018. Combined approaches to obtain cellulose nanocrystals, nanofibrils and fermentable sugars from elephant grass. Carbohydr. Polym. 180 (October 2017), 38–45.

Park, E.J., Jhon, D.Y., 2010. The antioxidant, angiotensin converting enzyme inhibition activity, and phenolic compounds of bamboo shoot extracts. LWT - Food Sci. Technol. (Lebensmittel-Wissenschaft -Technol.) 43 (4), 655–659.

Phanthong, P., Reubroycharoen, P., Hao, X., Xu, G., Abudula, A., Guan, G., 2018. Nanocellulose: extraction and application. Carbon Resour. Convers. 1 (1), 32–43.

Qing, W., Wang, Y., Wang, Y., Zhao, D., Liu, X., Zhu, J., 2016. The modified nanocrystalline cellulose for hydrophobic drug delivery. Appl. Surf. Sci. 366, 404–409.

Robles, E., Fernández-Rodríguez, J., Barbosa, A.M., Gordobil, O., Carreño, N.L.V., Labidi, J., 2018. Production of cellulose nanoparticles from blue agave waste treated with environmentally friendly processes. Carbohydr. Polym. 183 (October 2017), 294–302.

Silvério, H.A., Neto, W.P.F., Dantas, N.O., Pasquini, D., 2013. Extraction and characterization of cellulose nanocrystals from corncob for application as reinforcing agent in nanocomposites. Ind. Crops Prod. 44, 427–436.

Tan, X.Y., Abd Hamid, S.B., Lai, C.W., 2015. Preparation of high crystallinity cellulose nanocrystals (CNCs) by ionic liquid solvolysis. Biomass Bioenergy 81, 584–591.

Tang, J., Sisler, J., Grishkewich, N., Tam, K.C., 2017. Functionalization of cellulose nanocrystals for advanced applications. J. Colloid Interface Sci. 494, 397–409.

Teixeira, E., de, M., Bondancia, T.J., Teodoro, K.B.R., Corrêa, A.C., Marconcini, J.M., Mattoso, L.H.C., 2011. Sugarcane bagasse whiskers: extraction and characterizations. Ind. Crops Prod. 33 (1), 63–66.

Wang, Y., Wei, X., Li, J., Wang, F., Wang, Q., Chen, J., Kong, L., 2015. Study on nanocellulose by high pressure homogenization in homogeneous isolation. Fibers Polym. 16 (3), 572–578.

Wijaya, C.J., Saputra, S.N., Soetaredjo, F.E., Putro, J.N., Lin, C.X., Kurniawan, A., et al., 2017. Cellulose nanocrystals from passion fruit peels waste as antibiotic drug carrier. Carbohydr. Polym. 175, 370–376.

Xing, L., Gu, J., Zhang, W., Tu, D., Hu, C., 2018. Cellulose I and II nanocrystals produced by sulfuric acid hydrolysis of Tetra pak cellulose I. Carbohydr. Polym. 192 (February), 184–192.

Yang, Z., Zhang, M., Xin, D., Wang, J., Zhang, J., 2014. Evaluation of aqueous ammonia pretreatment for enzymatic hydrolysis of different fractions of bamboo shoot and mature bamboo. Bioresour. Technol. 173, 198–206.

Ye, L., Zhang, J., Zhao, J., Luo, Z., Tu, S., Yin, Y., 2015. Properties of biochar obtained from pyrolysis of bamboo shoot shell. J. Anal. Appl. Pyrolysis 114, 172–178.

Zainuddin, N., Ahmad, I., Kargarzadeh, H., Ramli, S., 2017. Hydrophobic kenaf nanocrystalline cellulose for the binding of curcumin. Carbohydr. Polym. 163, 261–269.

Zhang, F., Ran, C.X., Zheng, J., Ding, Y., Chen, G., 2018. Polysaccharides obtained from bamboo shoots (Chimonobambusa quadrangularis) processing by-products: new insight into ethanol precipitation and characterization. Int. J. Biol. Macromol. 112, 951–960.